Fast contribution to the activation energy of a glass-forming liquid

Tina Hecksher[a,1], Niels Boye Olsen[a], and Jeppe C. Dyre[a,1]

[a]Glass and Time, IMFUFA, Department of Science and Environment, Roskilde University, DK-4000 Roskilde, Denmark

Edited by Pablo G. Debenedetti, Princeton University, Princeton, NJ, and approved July 18, 2019 (received for review March 20, 2019)

This paper presents physical-aging data for the silicone oil tetramethyl-tetraphenyl trisiloxane. The density and the high-frequency plateau shear modulus G_∞ were monitored following temperature jumps starting from fully equilibrated conditions. Both quantities exhibit a fast change immediately after a temperature jump. Adopting the material-time formalism of Narayanaswamy, we determine from the dielectric loss at 0.178 Hz the time evolution of the aging-rate activation energy. The relative magnitude of the fast change of the activation energy differs from that of the density, but is identical to that of G_∞. In fact, the activation energy is proportional to G_∞ throughout the aging process, with minor deviations at the shortest times. This shows that for the silicone oil in question the dynamics are determined by G_∞ in—as well as out of—equilibrium.

physical aging | TN formalism | relaxation time activation energy

Physical aging is the term used for changes of material properties over time caused by adjustments of the positions of a system's atoms or molecules (1–16). Although aging and degradation of materials are often due to chemical reactions, physical aging is important for amorphous solids like polymers and oxide glasses during production as well as in subsequent use. The experimental study of physical aging requires measurements of high accuracy and considerable patience; simulations of aging are likewise demanding in terms of computational power requirements (17–19). Aging has been studied by monitoring density (1), enthalpy (2, 3), dc and ac electrical response (20–22), etc. Interestingly, these and other quantities all age in a very similar fashion.

Property changes due to physical aging rarely follow a simple exponential function in time, and even temperature changes as small as 1% usually lead to a response that is far from linear. Physical aging can only be observed just below the system's glass transition temperature because at lower temperatures, aging takes place on geological time scales. Many studies of physical aging monitor a quantity during and after the system's glass transition (2–4, 7, 14). A conceptually simpler case involves first equilibrating the system at one temperature by long-time annealing, after which the temperature is changed rapidly to a new, constant value where the full approach to equilibrium is monitored as a function of time. This is referred to as an ideal temperature-jump experiment if no relaxation takes place before the temperature is constant throughout the sample and if the system is monitored until equilibrium has been reached (21, 23). We report below close-to-ideal temperature-jump aging data for a silicone oil.

The Material Time and Single-Parameter Aging

A breakthrough in the description of physical aging was made in 1971 by Ford Motor Company engineer O. S. Narayanaswamy (2). He showed that physical aging can be described by a standard linear-response-theory–type convolution integral if the integration variable is changed from time to a so-called "material time," the rate of change of which itself evolves as the structure ages (2). This finding is still not fully understood theoretically (24). Yet, what became known as the Tool–Narayanaswamy (TN) aging formalism has been used in industry for decades. An excellent introduction to the TN formalism can be found in Scherer's 1986 textbook (7); we use this theoretical framework below to interpret data for the physical aging of the silicone oil DC704 (tetramethyl-tetraphenyl trisiloxane) in temperature-jump experiments.

Consider a temperature jump that starts from a state of equilibrium at the temperature $T_0+\Delta T$ and changes temperature to T_0 at $t=0$. If the quantity monitored is denoted by $X(t)$ and $\Delta X(t)$ is $X(t)$ minus its equilibrium value at T_0, the normalized relaxation function $R(t)$ is defined by

$$R(t) \equiv \Delta X(t)/\Delta X(0)\,. \qquad [1]$$

By construction, $R(0^-)=1$ (just before the jump) and $R(t\to\infty)=0$. For a temperature down jump, the system is self-retarded because the structure approaches one of slower structural relaxation. For a temperature up jump, the system is self-accelerated because the structure converges to one of faster relaxation (19, 25–27). Consequently, temperature down jumps result in relaxation functions that approach equilibrium faster and are more "stretched" than those of temperature up jumps to the same temperature, compare the red and blue curves in Fig. 1*B*.

According to Narayanaswamy, a glass-forming liquid has what may be thought of as an "internal" clock that quantifies how fast molecular rearrangements take place (2, 7, 28). In equilibrium, the clock rate is constant and equal to the inverse of the structural (alpha) relaxation time. In an aging system, the clock rate changes with time. If the material time is denoted by ξ, at any given time t the aging (clock) rate $\gamma(t)$ is defined by

Significance

One of the main questions in glass science is what causes the spectacular temperature dependence of the dynamics of a supercooled liquid. Answering this would establish the fundamental physics of glass-forming liquids and, in particular, settle the long-standing controversy about whether or not the relaxation time diverges at a finite temperature. This paper reports experiments on a glass-forming silicone oil, monitoring how the system equilibrates after temperature jumps carried out just below the glass-transition temperature. We find that the high-frequency shear modulus G_∞ and the activation energy of the relaxation time are proportional throughout the approach to equilibrium. Since G_∞ cannot diverge, this indicates that the relaxation time is finite at all temperatures.

Author contributions: N.B.O. designed research; T.H., N.B.O., and J.C.D. performed research; T.H. analyzed data; and T.H. and J.C.D. wrote the paper.

The authors declare no conflict of interest.

This article is a PNAS Direct Submission.

[1]To whom correspondence may be addressed. Email: tihe@ruc.dk or dyre@ruc.dk.

This article contains supporting information online at www.pnas.org/lookup/suppl/doi:10.1073/pnas.1904809116/-/DCSupplemental.

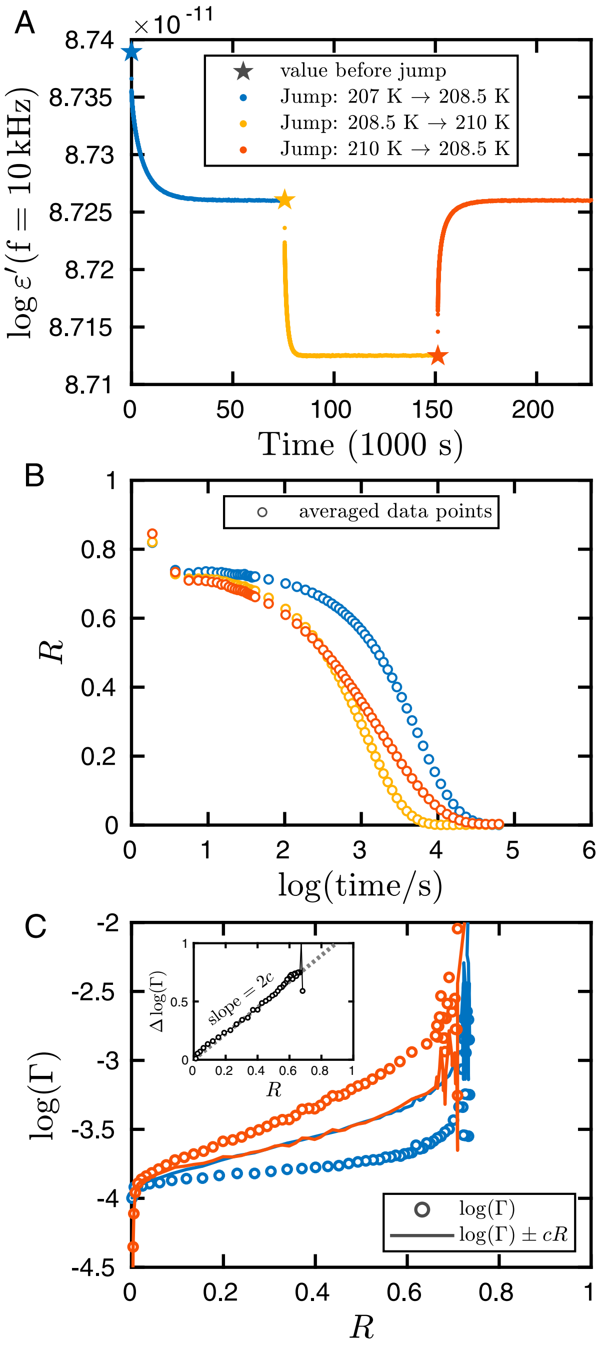

Fig. 1. Physical aging of the density of the silicone oil DC704 monitored by measuring the real part of the dielectric constant at 10 kHz after temperature jumps. Temperature is controlled by a Peltier element; due to the thin liquid layer (50 μm), the setup allows for temperature equilibration within a few seconds (21). (*A*) Data for 3 consecutive 1.5-K temperature jumps plotted as a function of time. (*B*) The corresponding normalized relaxation functions $R(t)$ vs. the logarithm (base 10) of the time after each jump. Since $\varepsilon'(f = 10\text{ kHz})$ is a linear function of the density (22, 33, 34), the 3 normalized relaxation functions are identical to the those of the density. The 2 temperature up jumps (blue and yellow) result in curves of the same shape, reflecting the principle of thermorheological simplicity (time aging–time superposition) (2, 7). (*C*) Test of the SPA prediction that the KM aging rate $\Gamma(t)$ (Eq. **5**) for down/up jumps to the same temperature obeys $\Gamma(R) = \Gamma_{\mathrm{lin}}(R)\exp(\pm kR)$ in which $\Gamma_{\mathrm{lin}}(R)$ is the linear KM aging rate, i.e., its $\Delta T \to 0$ limit. *C, Inset* validates this by plotting as a function of R the difference of the logarithms of the KM aging rates of the 2 jumps, $\Delta \log \Gamma$, resulting in a straight line. The main plot shows that the 2 relaxation curves superpose when compensated for the exponential R dependence (solid curves)—these curves give $\Gamma_{\mathrm{lin}}(R)$.

$$\gamma(t) \equiv \frac{d\xi}{dt}\,. \tag*{[2]}$$

The TN formalism (2, 7) predicts that upon a temperature jump carried out at $t = 0$, the normalized relaxation function is given by

$$R(t) = \phi(\xi)\,. \tag*{[3]}$$

Here $\xi = \xi(t)$ is the material time since the jump and, crucially, the function $\phi(\xi)$ is the same for all jumps. If $\phi(\xi)$ is a stretched exponential function, the above is referred to as the Tool–Narayanaswamy–Moynihan (TNM) description (29, 30). An attempt to justify TN was given in ref. 24, linking to previous work by Cugliandolo and Kurchan (31) who in the 1990s independently developed a closely related theory in the context of spin glasses.

The simplest case is that of single-parameter aging (SPA) (2, 7, 32). To introduce this concept, we write for any 2 physical quantities $X_1 \approx X_2$ if one is a linear function of the other in the relevant experimental range, i.e.,

$$X_1 \approx X_2 \Leftrightarrow X_1 = \alpha_{12} + \beta_{12} X_2\,. \tag*{[4]}$$

This defines an equivalence relation (recall from mathematics that $x \sim y$ is an equivalence relation if the following applies for all x, y, z: 1) $x \sim x$, 2) $x \sim y$ implies $y \sim x$, and 3) $x \sim y$ and $y \sim z$ implies $x \sim z$). In equilibrium, by first-order Taylor expansions all quantities are equivalent if only small temperature variations are considered. For 2 quantities to be regarded as equivalent in the present context, however, Eq. **4** must apply also for out-of-equilibrium conditions.

Since relaxation phenomena are generally thermally activated, we write the aging rate in terms of a time-dependent activation energy as follows: $\gamma(t) = \gamma_0 \exp[-\Delta E(t)/k_B T(t)]$ in which $\gamma_0 = 10^{14}\,\mathrm{s}^{-1}$ is the attempt frequency. By definition, a quantity X obeys SPA if $X \approx \Delta E$, in which case the aging rate at any given time is determined by $X(t)$ and the temperature (32).

Fig. 1*A* shows data for the aging of DC704 monitored by measuring the real part of the high-frequency dielectric constant, $\varepsilon'(f = 10\text{ kHz})$, after 2 consecutive 1.5-K temperature up jumps starting at 207.0 K, followed by a 1.5-K down jump. After each jump equilibrium is reached to a very good approximation so these are close-to-ideal temperature jumps. In the temperature range monitored $\varepsilon'(f = 10\text{ kHz})$ is almost frequency independent and, to a very good approximation, a linear function of the system's density ρ (33). Thus the normalized density relaxation function is identical to that of $\varepsilon'(f = 10\text{ kHz})$. This provides a convenient way to probe even small density changes (22, 33, 34). Fig. 1*B* shows the 3 normalized relaxation functions plotted as a function of the logarithm of the time since the jump. Comparing the up and down jumps to 208.5 K, blue and red, respectively, demonstrates the above-mentioned nonlinear nature of physical aging even for small temperature jumps.

Fig. 1*C* shows the Kovacs–McKenna (KM) aging rate defined (1, 28) by

$$\Gamma(t) \equiv -\frac{d \ln R(t)}{dt} \tag*{[5]}$$

plotted as a function of R for the up and down jumps ending at 208.5 K. The SPA assumption implies that $\gamma(t) = \gamma_{\mathrm{eq}} \exp(\pm kR(t))$ in which γ_{eq} is the equilibrium inverse relaxation time at 208.5 K and k is a numerical constant proportional to ΔT (32). The plus case represents the down jump from 210.0 K and the minus case describes the up jump from 207.0 K.

Eqs. **2**, **3**, and **5** imply for the Kovacs–McKenna aging rate $\Gamma(t) = -d\ln\phi/dt = -(d\ln\phi/d\xi)(d\xi/dt) = -[\phi'(\xi)/\phi(\xi)]\,\gamma(t) = -[\phi'(\xi)/\phi(\xi)]\gamma_{\mathrm{eq}} \exp[\pm kR(t)]$ in which $\xi = \xi(t)$. Since ξ by Eq. **3** is the same function of R for all jumps, one has by inversion $\xi = \xi(R)$. SPA thus predicts that for a given value of R, the ratio of the down- and up-jump KM aging rates is an exponential function of R. This is validated in Fig. 1*C*, *Inset*, which shows that the difference of the logarithms of the 2 KM aging rates is a linear function of R.

The 2 solid collapsing curves in the main plot in Fig. 1*C* show the density KM aging rates compensated for the exponential R dependence. This gives the KM aging rate predicted for an infinitesimal temperature jump, $\Gamma_{\mathrm{lin}}(R)$, corresponding to $k=0$ in the SPA characterizing equation $\gamma(t)=\gamma_{\mathrm{eq}}\exp(\pm kR(t))$. The solid curves are not horizontal because even linear aging is nonexponential, i.e., has a nonconstant KM aging rate.

The density data in Fig. 1 conform to the SPA prediction of a linear relation between the activation energy and the property measured; for DC704 this has also been established for the high-frequency shear-mechanical plateau modulus G_∞ (32). We show below, however, that this does not necessarily imply that Eq. **4** is obeyed because the same prediction applies for a more general version of SPA (Eq. **6**). Recently, glycerol was also shown to conform to the SPA prediction (35), which is interesting because hydrogen-bonding systems are generally more complex than van der Waals bonded systems.

A major challenge in glass science is what determines the activation energy of the dynamics of supercooled liquids. Is it the configurational entropy as in the Adam–Gibbs model from 1965 (36, 37) and later more sophisticated theories (38, 39)? Is it the density as in free-volume models (40, 41)? Is it the high-frequency plateau shear modulus G_∞ as in the shoving and related elastic models (42, 43)? Or is the activation energy not related to any well-known physical property? Answering these questions would put the fundamental physics of glass-forming liquids on a firm ground and, in particular, settle the long-standing controversy about whether or not the relaxation time of a glass-forming liquid diverges at a finite temperature (44–48). Before addressing how to determine the aging-rate activation energy, we compare the normalized relaxation functions of density and G_∞.

Comparing Density and G_∞ Aging

Fig. 2*B* compares the normalized relaxation functions of ρ and G_∞ for small temperature jumps. The density data represent the linearized overlapping solid curves in Fig. 1*C*; the G_∞ data are from resonance-frequency measurements for which aging following a temperature jump of just 0.15 K may be probed with good resolution (Fig. 2*A*). Fig. 2*B* shows that ρ and G_∞ both experience a fast change. This initial fast jump is significantly larger for ρ than for G_∞, however. Fig. 2*B*, *Inset* shows that after rescaling the 2 relaxation curves superpose.

The different magnitudes of the fast changes right after $t=0$ show that both quantities cannot obey SPA (Eq. **4**) because $\Delta E\approx\rho$ and $\Delta E\approx G_\infty$ leads to $\rho\approx G_\infty$, implying identical normalized relaxation functions for ρ and G_∞. The single-parameter aging tests in Fig. 1*C* and ref. 32 relate only to the relaxing part of the quantity X monitored, however, and these tests apply also if ΔE is equivalent to X in the more general sense

$$X_1\sim X_2 \Leftrightarrow X_1=\alpha_{12}(T)+\beta_{12}X_2\,. \qquad \textbf{[6]}$$

This allows for independent fast contributions of X_1 and X_2 upon a temperature jump. We henceforth say the quantity X obeys "rigorous SPA" if $\Delta E\approx X$ (Eq. **4**) and "general SPA" if the more general relation $\Delta E\sim X$ of Eq. **6** applies.

Determining the Aging-Rate Activation Energy

Fig. 2*B* showed that ρ and G_∞ cannot both be equivalent to ΔE in the sense of Eq. **4**, i.e., at most one of them obeys rigorous SPA. To investigate this more closely, one needs to find the aging-rate activation energy, which is done by arguing as follows (21). Fig. 3*A* shows the equilibrium dielectric loss of DC704 at 2 temperatures above the glass transition. The loss-peak frequency is identified with the equilibrium aging rate. If temperature is lowered, the equilibrium loss curve moves to lower frequencies. Fig. 3*A* illustrates the so-called shift-factor method of determining the aging rate $\gamma(t)$ (1, 5), which identifies $\gamma(t)$ by monitoring the dielectric loss at a fixed frequency f_c above the loss-peak frequency (vertical arrow) (21). DC704 obeys time–temperature superposition (TTS); moreover, DC704 has no measurable beta process (50) and a high-frequency loss that follows an approximate power law $\propto f^{-a}$ [$a\cong 0.5$ (51)]. From these facts, assuming the so-called time-aging–time-superposition property that is a prerequisite of the TN formalism (7, 52), it follows that $\gamma(t)$ during aging may be identified from $a\ln\gamma(t)=\ln\varepsilon''(f_c,t)+\mathrm{Const.}$ (21). Fig. 3*B* validates this method of determining the aging rate by showing that it predicts equilibrium aging rates consistent with

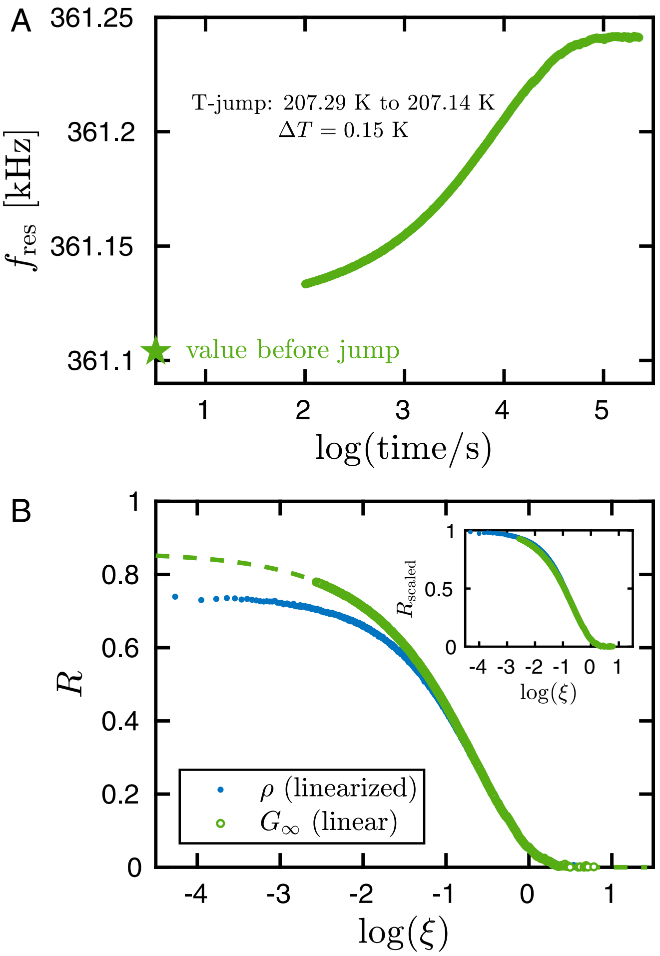

Fig. 2. Aging of the high-frequency plateau modulus G_∞ and the density ρ. (*A*) Resonance frequency f_{res} of a piezo-ceramic disc with DC704 sandwiched between the disc and a metal cylinder, which determines G_∞ by the expression $G_\infty = Af_{\mathrm{res}}^2 - B$ in which A and B are constants (see *SI Appendix* for how these constants are determined) (49). The resonance frequency is shown as a function of time after a temperature down jump of magnitude 0.15 K, which is small enough to be virtually linear. The temperature is stabilized and uniform throughout the sample after about 100 s. (*B*) The normalized relaxation function of G_∞ (green circles) and of the linearized density relaxation data in Fig. 1*C*. The fast contributions to the 2 normalized relaxation functions differ, implying that at most 1 of the 2 quantities can be equivalent to the activation energy in the sense of Eq. **4**. *B*, *Inset* shows that the 2 curves superpose when scaled empirically. This is consistent with the general single-parameter aging scenario for ρ and G_∞ defined by $\Delta E\sim X$ (Eq. **6**) in which X is the quantity monitored.

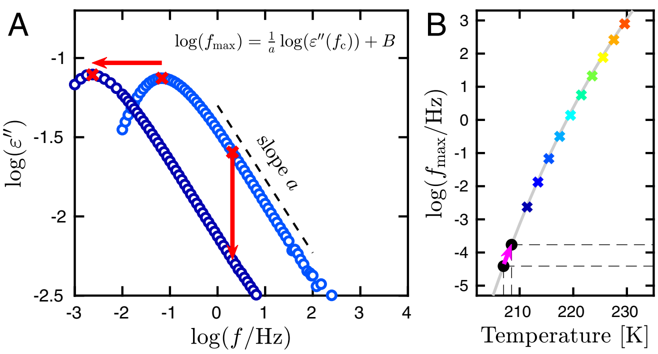

Fig. 3. Shift-factor method for determining the aging rate $\gamma(t)$. *A* shows the principle of the method, which utilizes the fact that DC704 has no beta relaxation and a high-frequency alpha dielectric loss varying as an inverse power law $\propto f^{-a}$ in which f is the frequency. In equilibrium, the logarithm of the dielectric loss measured at a fixed frequency f_c much above the loss peak (vertical arrow) is a linear function of the logarithm of the loss-peak frequency $f_{\max}$. This identifies the aging (relaxation) rate in equilibrium; the TN formalism implies that this method identifies the aging rate also in nonequilibrium situations (21). *B* demonstrates that the equilibrium rates obtained in this way are consistent with extrapolations of higher-temperature equilibrium loss-peak frequencies; the black circles show the initial and final values of the aging rate for the 207.0-K to 208.5-K jump.

extrapolations of higher-temperature equilibrium loss-peak data (black circles).

Due to the time it takes to establish a spatially constant temperature profile in our measuring cell after a jump, G_∞ can only be evaluated reliably for times longer than 100 s. Fig. 4*A* shows the aging-rate activation energy $\Delta E(t)$ following a jump from 207.0 K to 208.5 K, evaluated assuming $\gamma(t) = \gamma_0 \exp[-\Delta E(t)/k_B T(t)]$ in which $T(t) = 208.5$ K. Initially, there is a fast change of the activation energy. This is consistent with the recent finding by Niss (22) for polyisobutylene 625, which also showed a fast change in the activation energy. Fig. 4*C* compares the normalized relaxation function of the activation energy to that of the G_∞ aging data (Fig. 4*B*). The 2 curves superpose to a good approximation.

Is the activation energy proportional to the plateau modulus G_∞ as in the shoving model (42, 43)? The above analysis allows for $\alpha \neq 0$ in Eq. **4** in which case $\Delta E \propto G_\infty$ does not apply. Fig. 5 investigates more closely the relation between ΔE and G_∞. Fig. 5*A* plots the change of the activation energy from its equilibrium value at the starting temperature divided by the same for G_∞, showing that the 2 changes are proportional to a good approximation. This is confirmed by plotting in Fig. 5*B* the same ratio where instead the long-time limits were subtracted. Finally, Fig. 5*C* demonstrates directly that $\Delta E(t) \propto G_\infty(t)$ throughout the aging process with a minor deviation at the shortest times.

Thermodynamic Description of General Single-Parameter Aging

A single-parameter description of linear scalar thermoviscoelasticity was proposed some time ago, based on the following reasoning (53, 54). If temperature and pressure are externally controlled, each of their complementary variables entropy and volume is a linear combination of the temperature and pressure deviations from equilibrium plus a relaxing variable, i.e., a quantity that cannot change abruptly and which contains all memory of the thermal prehistory. A single-parameter description applies if the 2 relaxing variables are proportional in their time variation (53).

According to the Narayanaswamy recipe, linear scalar thermoviscoelasticity generalizes to the nonlinear case by replacing time by the material time. In the spirit of SPA it is reasonable to expect that the aging-rate activation energy is also a linear combination of temperature, pressure, and the relaxing variable. By expressing the latter in terms of volume, temperature, and pressure, a description of general SPA is arrived at which involves the system's temperature T, pressure p, and density ρ. Considering only small variations as in the above experiments, a thermodynamic description of general SPA is thus (5, 6, 55)

$$\Delta(\Delta E) = A\Delta T + B\Delta p + C\Delta\rho\,. \tag{7}$$

This "$Tp\rho$ model" is understood as follows. If the equilibrium reference state point has activation energy ΔE_0, temperature T_0, pressure p_0, and density ρ_0, the aging-rate activation energy as

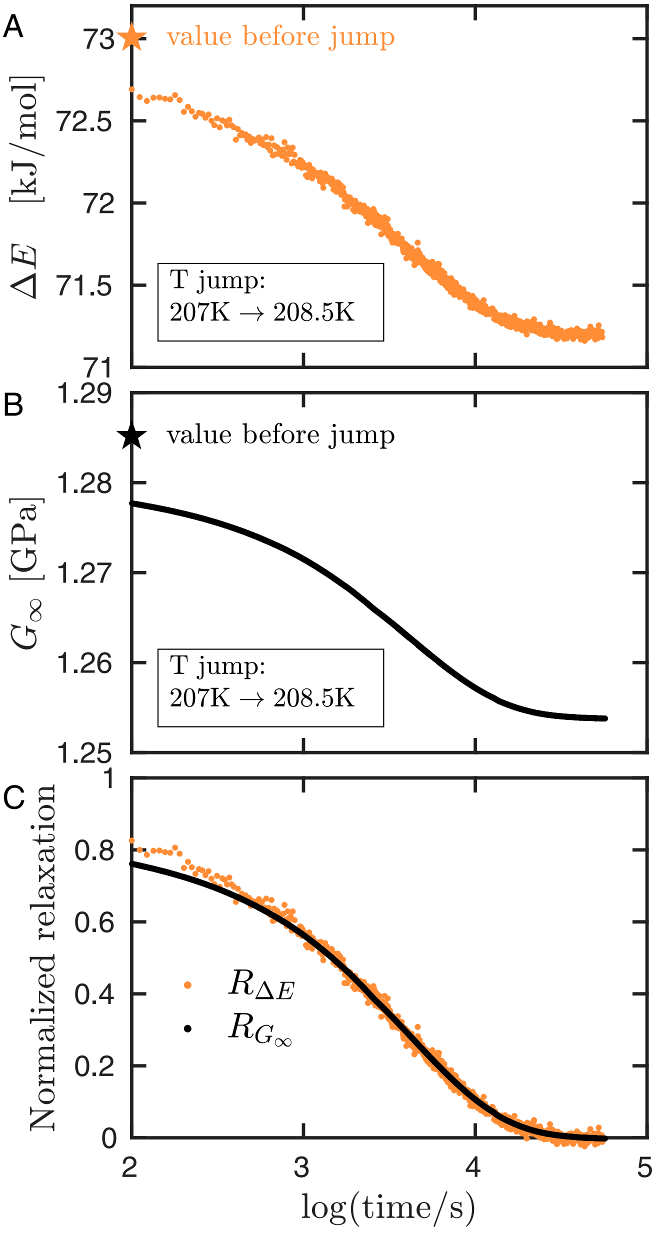

Fig. 4. Time development of the activation energy and G_∞ after a 1.5-K temperature up jump starting at 207.0 K. *A* shows the aging-rate activation energy as a function of time. The star on the *y* axis marks the equilibrium activation energy at the initial temperature. *B* shows G_∞ as a function of time for the same jump. *C* compares the normalized relaxation functions of the 2 quantities.

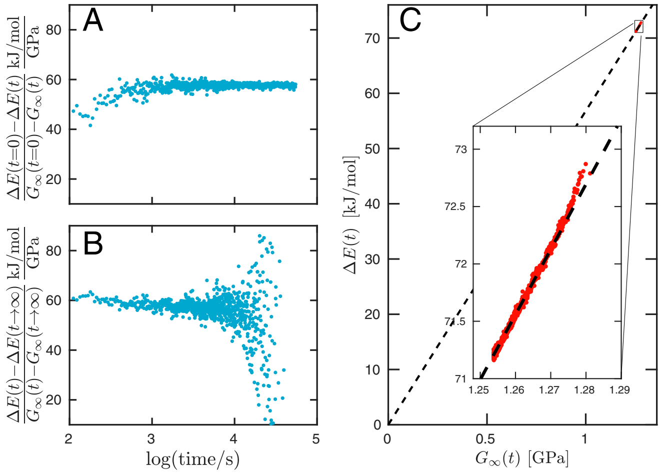

Fig. 5. Comparing the aging-rate activation energy to G_∞ for 207.0-K to 208.5-K temperature up jumps. *A* shows the change of the activation energy from its initial (equilibrium) value divided by the same change for G_∞ plotted as a function of time. The plot, which focuses on deviations from the initial values, shows a ratio that is constant in time. *B* shows the same ratio for the difference to the long-time limiting values. The noise at long times derives from the experimental uncertainties in the subtraction of almost identical values. *C* plots G_∞ vs. the activation energy where the dashed line marks proportionality. This plot demonstrates that $\Delta E \propto G_\infty$ during the aging process, with a minor deviation at the shortest times (compare *A*).

a function of the material time ξ is given by $\Delta E(\xi) - \Delta E_0 = A(T(\xi) - T_0) + B(p(\xi) - p_0) + C(\rho(\xi) - \rho_0)$. Note that most glass-forming liquids are "super-Arrhenius" in which case $A < 0$.

In ambient-pressure experiments $\Delta p = 0$ and Eq. **7** reduces to $\Delta(\Delta E) = A\Delta T + C\Delta\rho$. Consider a temperature jump to the reference state point, starting from equilibrium at $T_0 + \Delta T$. Before the jump the density is $\rho_0 + \Delta\rho$ in which $\Delta\rho = -\rho_0\alpha_p\Delta T$ where α_p is the isobaric thermal expansion coefficient. Thus before the jump the activation energy is $\Delta E_0 + (A - C\rho_0\alpha_p)\Delta T$. After the jump $T(\xi) = T_0$ and the activation energy is given by $\Delta E(\xi) = \Delta E_0 + C(\rho(\xi) - \rho_0) = \Delta E_0 - C\rho_0(\alpha_p - \alpha_p(\xi))\Delta T$ in which $\alpha_p(\xi)$ is the time-dependent isobaric thermal expansion coefficient ($\alpha_p = \alpha_p(\xi \to \infty)$). Thus the normalized relaxation function of the activation energy is for $\xi > 0$, i.e., after the fast change

$$R_{\Delta E}(\xi) = \frac{\alpha_p - \alpha_p(\xi)}{-A/(C\rho_0) + \alpha_p}\,. \qquad \textbf{[8]}$$

For comparison, the normalized density relaxation function is

$$R_\rho(\xi) = (\alpha_p - \alpha_p(\xi))/\alpha_p\,. \qquad \textbf{[9]}$$

The 2 functions are proportional for $\xi > 0$ and can be scaled to identical functions of the material time (and therefore also of the actual time).

Recently Niss (22) presented high-precision data for the aging rate as a function of volume for polyisobutylene 625 subjected to a number of different temperature jumps at ambient pressure (lower part of figure 2a in ref. 22). These data conform to the $Tp\rho$ model (Eq. **7**). Struik's (5) old polymer shift-factor aging data also obey Eq. **7** to a good approximation (figure 85 in ref. 5). For R-simple systems, i.e., those obeying hidden scale invariance believed to include most van der Waals liquids and metals (56), because of the strong correlations between virial and potential energy, Eq. **7** implies that besides temperature and density, the potential energy determines the aging-rate activation energy. This is the main assumption of the potential-energy-clock model of Adolf et al. (57, 58), which describes well several different experiments.

Concluding Remarks

We have introduced 2 versions of SPA for a quantity X monitored during aging, rigorous SPA defined by $\Delta E \approx X$ (Eq. **4**) and general SPA for which $\Delta E \sim X$ (Eq. **6**), which includes a term that follows the temperature instantaneously on the aging time scale. The density of the silicone oil DC704 obeys general SPA (Fig. 1) (32). The activation energy ΔE and G_∞ are found to be proportional throughout the aging toward equilibrium (Fig. 5*C*). This means that $\alpha = 0$ in the rigorous SPA aging condition $\Delta E \approx G_\infty$. We conclude that physical aging of DC704 is determined by G_∞.

Our findings for the out-of-equilibrium situation of physical aging are consistent with the shoving model for the equilibrium non-Arrhenius temperature dependence of the alpha relaxation time. According to this model, which describes the temperature dependence of the relaxation time of some but not all glass-forming liquids (59), the activation energy may be identified with the elastic work done locally on the surroundings to, for a brief moment, create the space needed for the molecules to rearrange (43, 60, 61).

Which function fits the aging data? The linear G_∞ aging data, which represent the single-parameter aging function $\phi(\xi)$, are well described by $\phi(\xi) = \exp(-c_1 - c_2\xi - c_3\sqrt{\xi})$ (*SI Appendix*). This function is the green dashed line in Fig. 2*B*. If $c_1 = c_2 = 0$, this corresponds to the TNM approach to aging based on the stretched exponential function $\phi(\xi) = \exp(-c_3\xi^\beta)$ with $\beta = 1/2$ (3).

A long-standing discussion in the field is whether or not the relaxation time of a metastable supercooled liquid diverges at a finite temperature (14, 36, 45, 62, 63). Prominent models like the Adam–Gibbs entropy model (36) and the more sophisticated random first-order theory (RFOT) of Wolynes and Lubchenko (64) predict such a divergence, while a recent related approach predicts a zero-temperature divergence of the relaxation time (65). Experimental evidence for a finite-temperature divergence has been reported (66), but other experiments question this conclusion (45, 48). The findings of this paper suggest that, at least for the silicone oil in question, the relaxation time does not diverge at a finite temperature because it is difficult to imagine that G_∞ diverges.

Our results imply that G_∞ is not a unique function of the density because if that were the case, density would also conform to rigorous SPA. This conclusion in conjunction with our finding that $\Delta E \approx G_\infty$ is consistent with high-pressure equilibrium experiments according to which isochoric relaxation is generally non-Arrhenius temperature dependent (67). On a more general note, we suggest that while high-pressure studies have been important for throwing light on the relaxation mechanism of supercooled liquids (54, 68), studies of physical aging at ambient pressure provide valuable additional information. For R-simple liquids, in particular, qualitatively new information is not obtained from high-pressure studies because structure and dynamics are invariant along the system's isomorphs. For such systems, studies of physical aging at ambient pressure like those presented here may provide a way forward for illuminating the long-standing puzzle of the origin of the non-Arrhenius temperature dependence of the relaxation time.

Materials and Methods

The setup used is described in *SI Appendix*.

ACKNOWLEDGMENTS. We are indebted to Kristine Niss for insightful discussions on aging over the years as well as her comments on the manuscript. Lisa Roed, Birthe Riechers, and Tage Christensen are also thanked for their comments on the manuscript. This work was supported by the VILLUM Foundation's grant Matter (16515).

1. A. J. Kovacs, Transition vitreuse dans les polymères amorphes. Etude phénoménologique. *Fortschr. Hochpolym.-Forsch.* **3**, 394–507 (1963).
2. O. S. Narayanaswamy, A model of structural relaxation in glass. *J. Am. Ceram. Soc.* **54**, 491–498 (1971).
3. C. T. Moynihan, A. J. Easteal, M. A. DeBolt, J. Tucker, Dependence of the fictive temperature of glass on cooling rate. *J. Am. Ceram. Soc.* **59**, 12–16 (1976).
4. O. Mazurin, Relaxation phenomena in glass. *J. Non-Cryst. Solids* **25**, 129–169 (1977).
5. L. C. E. Struik, *Physical Aging in Amorphous Polymers and Other Materials* (Elsevier, Amsterdam, The Netherlands, 1978).
6. A. J. Kovacs, J. J. Aklonis, J. M. Hutchinson, A. R. Ramos, Isobaric volume and enthalpy recovery of glasses. II. A transparent multiparameter theory. *J. Polym. Sci. Polym. Phys.* **17**, 1097–1162 (1979).
7. G. W. Scherer, *Relaxation in Glass and Composites* (Wiley, New York, NY, 1986).
8. I. M. Hodge, Physical aging in polymer glasses. *Science* **267**, 1945–1947 (1995).
9. J. M. Hutchinson, Physical aging of polymers. *Prog. Polym. Sci.* **20**, 703–760 (1995).
10. C. A. Angell, K. L. Ngai, G. B. McKenna, P. F. McMillan, S. W. Martin, Relaxation in glassforming liquids and amorphous solids. *J. Appl. Phys.* **88**, 3113–3157 (2000).
11. I. Kolvin, E. Bouchbinder, Simple nonlinear equation for structural relaxation in glasses. *Phys. Rev. E* **86**, 010501 (2012).
12. Y. P. Koh, S. L. Simon, Enthalpy recovery of polystyrene: Does a long-term aging plateau exist?*Macromolecules* **46**, 5815–5821 (2013).
13. D. Cangialosi, Dynamics and thermodynamics of polymer glasses. *J. Phys. Condens. Matter* **26**, 153101 (2014).
14. G. B. McKenna, S. L. Simon, 50th anniversary perspective: Challenges in the dynamics and kinetics of glass-forming polymers. *Macromolecules* **50**, 6333–6361 (2017).
15. B. Ruta, E. Pineda, Z. Evenson, Relaxation processes and physical aging in metallic glasses. *J. Phys. Condens. Matter* **29**, 503002 (2017).
16. D. Cangialosi, *Physical Aging of Polymers* (Wiley, 2018), pp. 1–36.
17. K. Vollmayr-Lee, W. Kob, K. Binder, A. Zippelius, Dynamical heterogeneities below the glass transition. *J. Chem. Phys.* **116**, 5158–5166 (2002).
18. H. E. Castillo, A. Parsaeian, Local fluctuations in the ageing of a simple structural glass. *Nat. Phys.* **3**, 26–28 (2007).
19. Z. W. Wu, W. Kob, W. H. Wang, L. Xu, Stretched and compressed exponentials in the relaxation dynamics of a metallic glass-forming melt. *Nat. Commun.* **9**, 5334 (2018).
20. P. Lunkenheimer, R. Wehn, U. Schneider, A. Loidl, Glassy aging dynamics. *Phys. Rev. Lett.* **95**, 055702 (2005).
21. T. Hecksher, N. B. Olsen, K. Niss, J. C. Dyre, Physical aging of molecular glasses studied by a device allowing for rapid thermal equilibration. *J. Chem. Phys.* **133**, 174514 (2010).
22. K. Niss, Mapping isobaric aging onto the equilibrium phase diagram. *Phys. Rev. Lett.* **119**, 115703 (2017).
23. S. Kolla, S. L. Simon, The τ-effective paradox: New measurements towards a resolution. *Polymer* **46**, 733–739 (2005).
24. J. C. Dyre, Narayanaswamy's 1971 aging theory and material time. *J. Chem. Phys.* **143**, 114507 (2015).
25. A. Q. Tool, Relation between inelastic deformability and thermal expansion of glass in its annealing range. *J. Am. Ceram. Soc.* **29**, 240–253 (1946).
26. J. C. Mauro, R. J. Loucks, P. K. Gupta, Fictive temperature and the glassy state. *J. Am. Ceram. Soc.* **92**, 75–86 (2009).
27. D. Cangialosi, V. M. Boucher, A. Alegria, J. Colmenero, Physical aging in polymers and polymer nanocomposites: Recent results and open questions. *Soft Matter* **9**, 8619–8630 (2013).
28. G. B. McKenna, On the physics required for prediction of long term performance of polymers and their composites. *J. Res. Natl. Inst. Stand. Technol.* **99**, 169–189 (1994).
29. C. T. Moynihan *et al.*, Structural relaxation in vitreous materials. *Ann. N. Y. Acad. Sci.* **279**, 15–35 (1976).
30. I. M. Hodge, A personal account of developments in enthalpy relaxation: A tribute to C. T. Moynihan. *J. Am. Ceram. Soc.* **91**, 766–772 (2008).
31. L. F. Cugliandolo, J. Kurchan, On the out-of-equilibrium relaxation of the Sherrington-Kirkpatrick model. *J. Phys. A Math. Gen.* **27**, 5749–5772 (1994).
32. T. Hecksher, N. B. Olsen, J. C. Dyre, Communication: Direct tests of single-parameter aging. *J. Chem. Phys.* **142**, 241103 (2015).
33. C. Bauer *et al.*, Capacitive scanning dilatometry and frequency-dependent thermal expansion of polymer films. *Phys. Rev. E* **61**, 1755–1764 (2000).
34. K. Niss, D. Gundermann, T. Christensen, J. C. Dyre, Dynamic thermal expansivity of liquids near the glass transition. *Phys. Rev. E* **85**, 041501 (2012).
35. L. A. Roed, T. Hecksher, J. C. Dyre, K. Niss, Generalized single-parameter aging tests and their application to glycerol. *J. Chem. Phys.* **150**, 044501 (2019).
36. G. Adam, J. H. Gibbs, On temperature dependence of cooperative relaxation properties in glass-forming liquids. *J. Chem. Phys.* **43**, 139–146 (1965).
37. I. M. Hodge, Adam-Gibbs formulation of enthalpy relaxation near the glass transition. *J. Res. Natl. Inst. Stand. Technol.* **102**, 195–205 (1997).
38. V. Lubchenko, P. G. Wolynes, Theory of aging in structural glasses. *J. Chem. Phys.* **121**, 2852–2865 (2004).
39. J. Dudowicz, K. F. Freed, J. F. Douglas, Generalized entropy theory of polymer glass formation. *Adv. Chem. Phys.* **137**, 125–222 (2008).
40. A. K. Doolittle, Studies in Newtonian flow. II. The dependence of the viscosity of liquids on free–space. *J. Appl. Phys.* **22**, 1471–1475 (1951).
41. M. H. Cohen, G. S. Grest, Liquid-glass transition, a free-volume approach. *Phys. Rev. B* **20**, 1077–1098 (1979).
42. J. C. Dyre, N. B. Olsen, T. Christensen, Local elastic expansion model for viscous-flow activation energies of glass-forming molecular liquids. *Phys. Rev. B* **53**, 2171–2174 (1996).
43. J. C. Dyre, The glass transition and elastic models of glass-forming liquids. *Rev. Mod. Phys.* **78**, 953–972 (2006).
44. W. Kauzmann, The nature of the glassy state and the behavior of liquids at low temperatures. *Chem. Rev.* **43**, 219–256 (1948).
45. T. Hecksher, A. I. Nielsen, N. B. Olsen, J. C. Dyre, Little evidence for dynamic divergences in ultraviscous molecular liquids. *Nat. Phys.* **4**, 737–741 (2008).
46. J. C. Mauro, Y. Yue, A. J. Ellison, P. K. Gupta, D. C. Allan, Viscosity of glass-forming liquids. *Proc. Natl. Acad. Sci. U.S.A.* **106**, 19780–19784 (2009).
47. L. Berthier, G. Biroli, Theoretical perspective on the glass transition and amorphous materials. *Rev. Mod. Phys.* **83**, 587–645 (2011).
48. G. B. McKenna, J. Zhao, Accumulating evidence for non-diverging time-scales in glass-forming fluids. *J. Non-Cryst. Solids* **407**, 3–13 (2015).
49. T. Christensen, N. B. Olsen, A rheometer for the measurement of a high shear modulus covering more than seven decades of frequency below 50 kHz. *Rev. Sci. Instrum.* **66**, 5019–5031 (1995).
50. T. Hecksher, K. Niss, Perspective: Searching for simplicity rather than universality in glass-forming liquids. *J. Chem. Phys.* **149**, 230901 (2018).
51. A. I. Nielsen *et al.*, Prevalence of approximate $\sqrt{t}$ relaxation for the dielectric α process in viscous organic liquids. *J. Chem. Phys.* **130**, 154508 (2009).
52. P. A. O'Connell, G. B. McKenna, Large deformation response of polycarbonate: Time-temperature, time-aging time, and time-strain superposition. *Polym. Eng. Sci.* **37**, 1485–1495 (1997).
53. N. L. Ellegaard *et al.*, Single-order-parameter description of glass-forming liquids: A one-frequency test. *J. Chem. Phys.* **126**, 074502 (2007).
54. D. Gundermann *et al.*, Predicting the density–scaling exponent of a glass–forming liquid from Prigogine–Defay ratio measurements. *Nat. Phys.* **7**, 816–821 (2011).
55. L. Grassia, A. D'Amore, Constitutive law describing the phenomenology of subyield mechanically stimulated glasses. *Phys. Rev. E*, **74**, 021504 (2006).
56. J. C. Dyre, Hidden scale invariance in condensed matter. *J. Phys. Chem. B* **118**, 10007–10024 (2014).
57. D. B. Adolf, R. S. Chambers, J. Flemming, Potential energy clock model: Justification and challenging predictions. *J. Rheol.* **51**, 517–540 (2007).
58. D. B. Adolf, R. S. Chambers, M. A. Neidigk, A simplified potential energy clock model for glassy polymers. *Polymer* **50**, 4257–4269 (2009).
59. T. Hecksher, J. C. Dyre, A review of experiments testing the shoving model. *J. Non-Cryst. Solids* **407**, 14–22 (2015).
60. W. Schirmacher, G. Ruocco, V. Mazzone, Heterogeneous viscoelasticity: A combined theory of dynamic and elastic heterogeneity. *Phys. Rev. Lett.* **115**, 015901 (2015).
61. B. Shang, J. Rottler, P. Guan, J. L. Barrat, Local versus global stretched mechanical response in a supercooled liquid near the glass transition. *Phys. Rev. Lett.* **122**, 105501 (2019).
62. F. H. Stillinger, Supercooled liquids, glass transitions, and the Kauzmann paradox. *J. Chem. Phys.* **88**, 7818–7825 (1988).
63. M. Ozawa, C. Scalliet, A. Ninarello, L. Berthier, Does the Adam-Gibbs relation hold in simulated supercooled liquids? arXiv:1905.08179 (20 May 2019).
64. P. G. Wolynes, V. Lubchenko, *Structural Glasses and Supercooled Liquids: Theory, Experiment, and Applications* (Wiley, 2012).
65. M. C. Angelini, G. Biroli, Real space renormalization group theory of disordered models of glasses. *Proc. Natl. Acad. Sci. U.S.A.* **114**, 3328–3333 (2017).
66. R. Richert, C. A. Angell, Dynamics of glass-forming liquids. V. On the link between molecular dynamics and configurational entropy. *J. Chem. Phys.* **108**, 9016–9026 (1998).
67. G. Tarjus, D. Kivelson, S. Mossa, C. Alba-Simionesco, Disentangling density and temperature effects in the viscous slowing down of glassforming liquids. *J. Chem. Phys.* **120**, 6135–6141 (2004).
68. C. M. Roland, S. Hensel-Bielowka, M. Paluch, R. Casalini, Supercooled dynamics of glass-forming liquids and polymers under hydrostatic pressure. *Rep. Prog. Phys.* **68**, 1405–1478 (2005).